

A GRANULAR EXPERIMENT APPROACH TO EARTHQUAKES

TERREMOTOS A TRAVÉS DE UN EXPERIMENTO CON GRANOS

S. LHERMINIER^{a†}, R. PLANET^a, G. SIMON^a, K.J. MÅLØY^b, L. VANEL^a, O. RAMOS^a

a) Institut Lumière Matière, UMR5306 Université Lyon 1-CNRS, Université de Lyon, 69622 Villeurbanne, France; sebastien.lherminier@univ-lyon1.fr[†]

b) Department of Physics, University of Oslo, P. O. Box 1048, 0316 Oslo, Norway

† corresponding author

Recibido 19/3/2015; Aceptado 19/4/2016

Although earthquakes have been scientifically studied for more than a century, essential questions as the possibility of predicting catastrophic events remain still open. Here we introduce an original experimental setup that mimics the behavior of a tectonic fault. By continuously shearing a granular layer under confined pressure, we are able to obtain a dynamics ruled by scale-invariant avalanches. We monitor the sizes of these avalanches by two methods and both show a power-law distribution (similar to the Gutenberg-Richter law). There is also a strong resemblance between waiting times distribution in our experiment and other studies with real earthquakes data.

Aunque los terremotos han sido estudiados científicamente durante más de un siglo, preguntas esenciales como la posibilidad de predecir eventos catastróficos permanecen todavía por resolver. Aquí introducimos un sistema experimental original que imita el comportamiento de una falla tectónica. Mediante el cizalle continuo de una capa granular sometida a una presión de confinamiento, somos capaces de obtener una dinámica de avalanchas invariantes de escala. Supervisamos los tamaños de estas avalanchas por dos métodos y ambos muestran una distribución en ley de potencia (similar a la ley de Gutenberg-Richter). Hay también una gran similitud entre la distribución de tiempos que espera entre eventos obtenidos en nuestro experimento y otros estudios con datos de terremotos reales.

PACS: Granular systems, 45.70.-n; avalanches, 45.70.Ht; earthquakes, 91.30.Px

I. INTRODUCTION

Most earthquakes occur at fault zones, where friction between two tectonic plates colliding or sliding against each other causes a stick-slip-like movement. During stick states, energy is stored as deformations in the rocks around the fault zone. Once the accumulated stress is enough to break through the asperities of the plates [1], the stored energy is released by unlocking of the fault: during a brief moment, the relative velocity of the plates is very high, until it locks again, generating an earthquake. In the case of large earthquakes, the consequences on human society can be catastrophic [2].

Earthquakes are classified by their size, using the well-known magnitude M , linked to the energy E of the earthquake by the relation $M = 2/3 \log(E) + K$, where K is a constant. The probability distribution of a series of earthquakes sorted by their energy is given by a power-law $P(E) \sim E^{-b}$ with an exponent $b = 5/3 = 1.66$, known as the Gutenberg-Richter (GR) law [3, 4]. This kind of behavior where sudden events have sizes distributed following a power law is called scale-invariance avalanches, and is rather common in nature. Scale-invariance avalanches have been reported in phenomena as diverse as snow avalanches [5], granular piles [6–10], solar flares [11, 12], superconducting vortices [13], sub-critical fracture [14, 15], evolution of species [16] and even stock market crashes [17, 18].

Even if considerable work has been done to understand the earthquakes dynamics — mainly from the Geophysical community but also from the general perspective of scale-invariant avalanches [19–23] — many issues remain as

open questions, and the essential fact about the possibility of predicting catastrophic quakes is still a subject of debate [22, 24].

In order to bring some answers to different open questions about earthquakes and scale-invariant phenomena in general, we present an original experimental setup that reproduces the behavior of a tectonic fault.

A fault is a planar fracture at the frontier between two plates, defining the direction of motion. The material physically separating the two plates is called the fault gouge and is composed of crushed rocks from the friction and wear between the two plates. The typical way of modeling the gouge is by using disks or spheres [25, 26], as a mean to reduce complexity.

As of today, the best attempts to reproduce the dynamics of earthquakes comes from friction or fracture experiments. Overcoming the static friction between two solid blocks under a controlled load [27, 28] is maybe the simplest example. In this case the study generally focuses on one single event. Other experiments have sheared a granular layer, trying to simulate the behavior of a tectonic fault. However, it has been difficult to obtain a distribution of events that resembles the Gutenberg-Richter law [3]. Sometimes because the intrinsic response of the system is a regular stick-slip with all “earthquakes” having approximately the same size [29] and sometimes because insufficient statistical sets of data [30, 31]: most of the recent shear experiments have a linear geometry. Consequently, the relative motion between the two sliders is limited to a fraction of the length of the system, which is responsible

for the insufficient data collection. In the case of fracture, analogous to both the GR and Omori law have been observed in subcritical fracture experiments [15,32]. However, fracture is by nature a non-stationary process and the characteristics of the system change as it accelerates towards total failure.

To go beyond these current limitations, an original setup has been built. It uses a 2D granular material to model the fault gouge, mainly responsible for the dynamics of a fault. The gouge is sheared between two rough surfaces at a constant and very low speed. Thanks to periodic boundary conditions, we have access to rich statistics and have been able to produce scale-invariant avalanches. This paper presents a few preliminary results of this laboratory “earthquake machine”.

II. EXPERIMENTAL SETUP

The experimental setup consists of two fixed, transparent, and concentric cylinders, with a gap between them, so that a monolayer of disks can be introduced into the gap (see Fig. 1). The disks have 4 mm thickness and 6.4 mm and 7.0 mm diameter (in equal proportion) to avoid crystallization.

They are made of Durus White 430 and have been generated in a Objet30 3D printer.

The translucent and photoelastic character of the grains allows the visualization of the stress inside the disks when placing the experimental setup between two circular polarizers (close-up in Fig. 1).

The Young’s modulus of Durus material is $E \approx 100 \text{ MPa}$, which contrasts with the classical experiments using photoelastic disks with a Young’s modulus $E = 4 \text{ MPa}$ [30, 31, 33–37]. Our grains can hold a much larger stress without a considerable deformation, which favors both the acoustic propagation and image analysis [38].

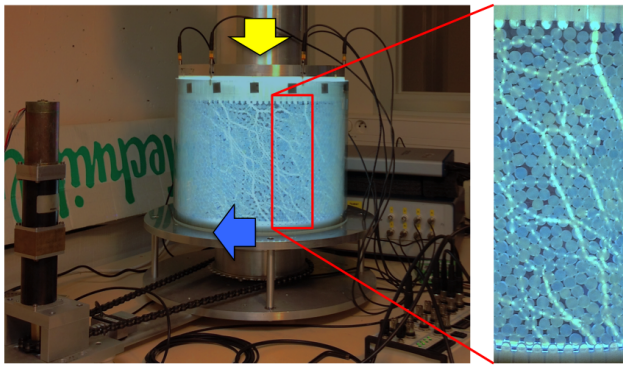


Figure 1. Experimental setup. The yellow and blue arrows represent the confining force and the shear direction respectively. (close-up) The birefringent nature of the material of the disks allows visualization of the internal force chains in the granular material

Two rings containing “fixed grains” constrain the pack from upper and bottom boundaries. The yellow arrow in Fig. 1 indicate the force between the plates, fixed by a dead load of 35 kg. As the rings rotate in relation to each other (blue arrow in Fig. 1) at a constant and very low speed ($7.6 \mu\text{m/s}$,

so 1 complete rotation every 36.7 hours), shear stresses build up on the packed beads.

The release of these stresses happens with sudden avalanches (*i.e.* reorganizations of the packing), and is also associated with acoustic emissions. In order to characterize the mechanical response of the sheared material we extract the resisting torque of the system using a steel lever and a force sensor Interface SML-900N (of range 900 N) sampled at 10 Hz. Acoustic measurements are performed using piezoelectric pinducers (VP-1.5 from CTS Valpey Corporation, sampled at 100 kHz) inserted in adjusted holes in the upper ring.

In this article we focus on the analysis of the resisting torque and the acoustic emissions.

III. RESULTS

The global mechanical response of the system shows a clear stick-slip-like behavior, since the measure of the resisting torque shows a continuous loading with intermittent drops of largely distributed sizes (see Fig. 2a). These drops are the signature of sudden global reorganizations of the pile, *i.e.* avalanches.

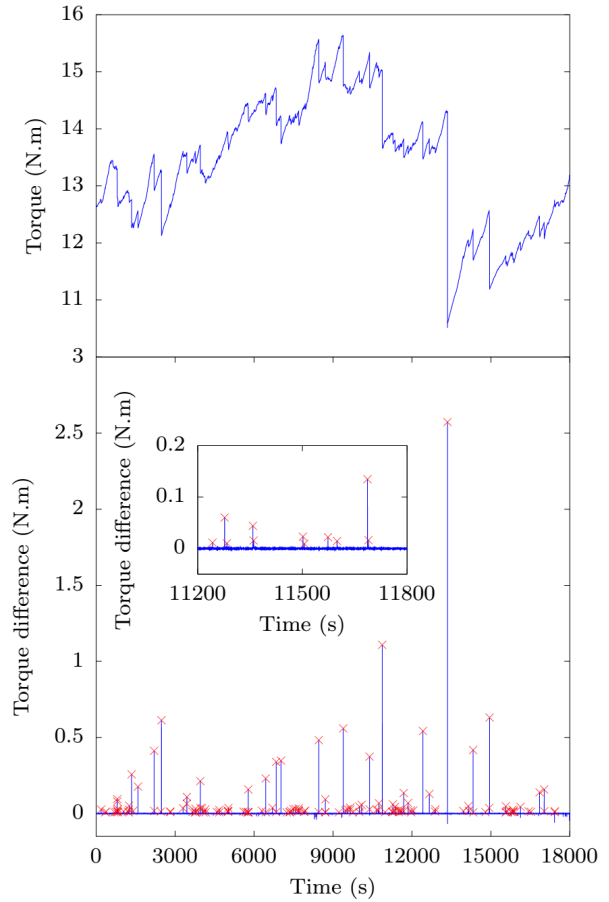


Figure 2. (a) Typical torque signal on a 5 hours time window. (b) Difference between two consecutive torque measurements shown in (a). Red crosses represent the detected events. The small events appear clearly when zooming (see the inset), even if they seemed invisible due to the large distribution of sizes.

The reorganization will begin with one grain exceeding its frictional threshold, moving, and thus releasing stress

over its neighbors. The phenomenon will propagate along neighbors until all the grains are friction-locked, hence the name avalanche.

This stress release will manifest itself by a very brief decrease of the applied torque on the top boundary.

Since the mechanical response is regularly sampled, the size of the avalanche can be extracted from the difference of the torque signal between two consecutive time steps (see Fig. 2b).

Avalanches will appear as peaks high over of the noise. Since the amplitudes of the peaks are largely distributed (over a few decades), it is necessary to zoom in on a portion of the signal to distinguish the smallest peaks. Since the velocity of the moving ring is very small (in average one event every 200 seconds), it is necessary to wait for long times to acquire enough statistics (typically a few days long).

We can then extract the probability distribution of the events' sizes, shown on Fig. 3. The distribution follows a power-law for small sizes and reaches a cutoff at large ones (over 10 N.m). The cutoff regime has low statistics (around 2 % of the total), so a precise behavior is hard to obtain. The power-law regime is characterized by an exponent 1.67 ± 0.04 computed from maximum likelihood method [39]. We here find a first similarity with real earthquakes by comparing this power-law regime with the GR law. However, we notice that here the exponent is computed for torque drops, where the GR law deals with energies of the earthquakes.

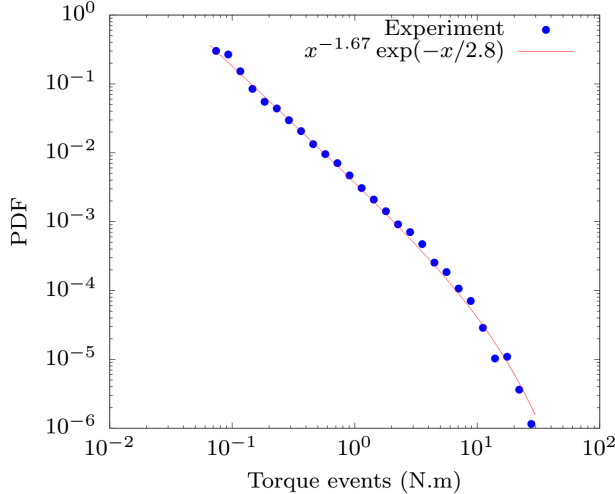


Figure 3. Avalanches size distribution from an 14 days experiment, representing $\sim 10,000$ events. We show the maximum likelihood fit with an exponentially-truncated power-law.

From acoustic measurements we are able to extract the energy of acoustic emissions, computed as the spectral energy (sum of spectral amplitudes in the bandwidth from 0.5 to 15 kHz, which include all the frequencies that have been observed during acoustic events) of the signal on the detected duration of the event. We observe again that the energy probability distribution scales as a power-law (see Fig. 4) with an exponent 1.72 ± 0.04 , again computed by maximum likelihood method. We are currently analyzing the relation between both measurements (torque and acoustics), as well

as the influence of the frequency of measurement, which may be a cause of the different exponent values obtained in the experiment [15].

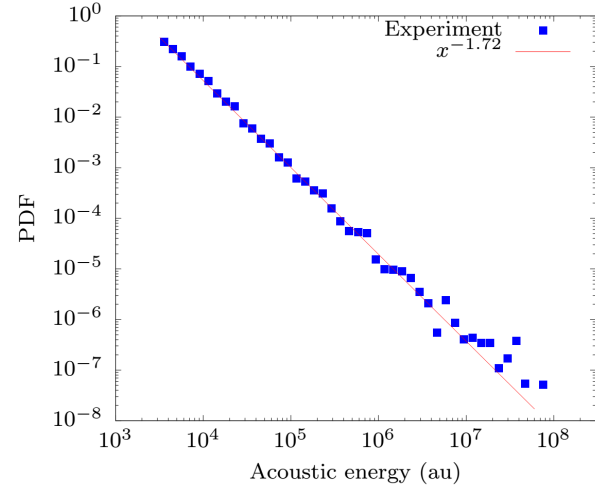


Figure 4. Acoustic energy distribution from a 1 day experiment, representing $\sim 6,000$ events. The maximum likelihood fit with a power-law is also shown.

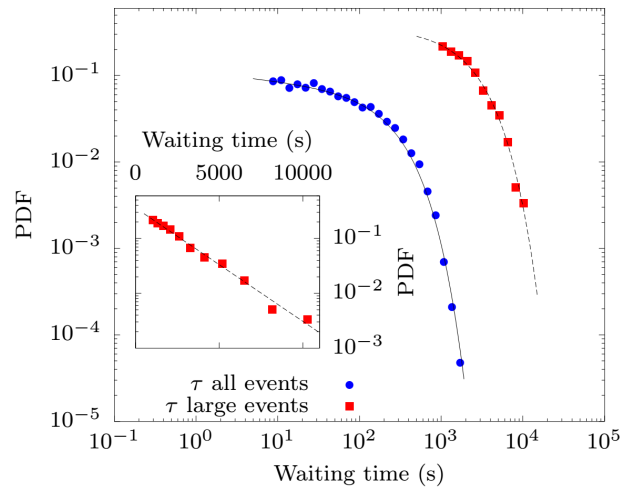


Figure 5. Waiting times probability distribution for the whole set of avalanches (●) with PDF shown in Fig. 3. The solid line (—) is a fit to the data of a generalized gamma distribution. The represented gamma distribution has the form $\tau^{-0.1} \exp(-\tau/256)$. The figure also shows the probability distribution (■) of waiting times for only large events (sizes greater than a tenth of the maximum event detected, representing $\sim 5\%$ of the events). The dashed line (---) is a fit to the data representing an exponential distribution characterized by $\exp(-\tau/2100)$. The inset shows the data for large events in semilog scale to highlight the exponential dependency.

A second characteristic of earthquakes is the distribution of waiting times between two events. We are able to compute these waiting times as well (see Fig. 5), both for the whole set of events and for only large ones (a large event has a size greater than a tenth of the maximum size, here 3 N.m). The behavior for the whole set of events is compatible with a generalized gamma function as found in [40]: the scaling extracted is of the form $\tau^{-\gamma} \exp(-\tau/\tau_0)$ with $\gamma = 0.10 \pm 0.02$ and $\tau_0 = 256 \pm 4$. If only the large events are taken into account, then an exponential behavior is obtained $\exp(-\tau/\tau_l)$ with $\tau_l = 2100 \pm 50$, which means we have a Poisson process

with independent large events, which is also the case in real earthquakes.

IV. CONCLUSIONS

In this paper we have presented a laboratory “earthquake machine” that generates scale-invariant avalanches with similar behavior than real earthquakes, by modeling the dynamics of a fault zone with a sheared 2D granular medium. Both the global mechanical response and acoustic emissions are monitored and both show scale-invariant avalanches. The probability distribution of events’ sizes are consistent with the Gutenberg-Richter law observed for real earthquakes. A study of waiting times between events is also consistent with behaviors observed by previous studies on real earthquakes.

We acknowledge financial support from AXA Research Fund.

REFERENCES

- [1] M. Ohnaka, *The Physics of Rock Failure and Earthquakes* (Cambridge University Press, 1993).
- [2] B. Bolt, *Earthquakes: Revised and Expanded* (W.H. Freeman and Company, New York, 1993).
- [3] B. Gutenberg and C. F. Richter, *Annali di Geofisica* 9, 1 (1956).
- [4] T. C. Hanks and H. Kanamori, *Journal of Geophysical Research: Solid Earth* 84, 2348 (1979).
- [5] K. W. Birkeland and C. C. Landry, *Geophysical Research Letters* 29, 49 (2002).
- [6] G. A. Held, D. H. Solina, H. Solina, D. T. Keane, W. J. Haag, P. M. Horn and G. Grinstein, *Phys Rev Lett* 65, 1120 (1990).
- [7] V. Frette, K. Christensen, A. Malthe-Sørenssen, J. Feders, T. Jøssang and P. Meakin, *Nature* 379, 49 (1996).
- [8] E. Altshuler, O. Ramos, C. Martínez, L. E. Flores and C. Noda, *Phys Rev Lett* 86, 5490 (2001).
- [9] C. M. Aegerter, K. A. Lörincz, M. S. Welling and R. J. Wijngaarden, *Phys Rev Lett* 92, 058702 (2004).
- [10] O. Ramos, E. Altshuler and K. J. Måløy, *Phys Rev Lett* 102, 078701 (2009).
- [11] B. R. Dennis, *Solar Physics* 100, 465 (1985).
- [12] D. Hamon, M. Nicodemi and H. J. Jensen, *Astronomy and Astrophysics* 387, 326 (2002).
- [13] E. Altshuler and T. H. Johansen, *Rev Mod Phys* 76, 471 (2004).
- [14] S. Santucci, L. Vanel and S. Ciliberto, *Phys. Rev. Lett.* 93, 095505 (2004).
- [15] M. Stojanova, S. Santucci, L. Vanel and O. Ramos, *Phys. Rev. Lett.* 112, 115502 (2014).
- [16] K. Sneppen, P. Bak, H. Flyvbjerg and M. H. Jensen, *Proceedings of the National Academy of Sciences* 92, 5209 (1995).
- [17] Y. Lee, L. A. Nunes Amaral, D. Canning, M. Meyer and H. E. Stanley, *Phys. Rev. Lett.* 81, 3275 (1998).
- [18] X. Gabaix, P. Gopikrishnan, V. Plerou and H. E. Stanley, *Nature* 423, 267 (2003).
- [19] P. Bak, C. Tang and K. Wiesenfeld, *Phys. Rev. Lett.* 59, 381 (1987).
- [20] P. Bak, *How Nature works-The Science of Self-organized Criticality* (Oxford Univ. Press, Oxford, 1997).
- [21] H. J. Jensen, *Self-organized Criticality, Emergent Complex Behavior in Physical and Biological Systems* (Cambridge Univ. Press, Cambridge, 1998).
- [22] I. Main, *Nature* (1999).
- [23] O. Ramos, B. Veress and J. Szigethy, eds., *Horizons in Earth Science Research. Vol. 3* (Nova Science Publishers, 2011).
- [24] R. J. Geller, D. D. Jackson, Y. Y. Kagan and F. Mulargia, *Science* 275, 1616 (1997).
- [25] F. Alonso-Marroquín, I. Vardoulakis, H. J. Herrmann, D. Weatherley and P. Mora, *Phys. Rev. E* 74, 031306 (2006).
- [26] S. Abe, S. Latham and P. Mora, *Pure and applied geophysics* 163, 1881 (2006), ISSN 0033-4553.
- [27] O. Ben-David, G. Cohen and J. Fineberg, *Science* 330, 211 (2010).
- [28] S. M. Rubinstein, G. Cohen and J. Fineberg, *Phys. Rev. Lett.* 98, 226103 (2007).
- [29] P. A. Johnson, H. Savage, M. Knuth, J. Gombeg and C. Marone, *Nature* 451, 57 (2008).
- [30] K. E. Daniels and N. W. Hayman, *Journal of Geophysical Research: Solid Earth* 113, 2156 (2008).
- [31] D. M. Walker, A. Tordesillas, M. Small, R. P. Behringer and C. K. Tse, *Chaos: An Interdisciplinary Journal of Nonlinear Science* 24, 013132 (2014).
- [32] J. Baró, A. Corral, X. Illa, A. Planes, E. K. H. Salje, W. Schranz, D. E. Soto-Parra and E. Vives, *Phys. Rev. Lett.* 110, 088702 (2013).
- [33] B. Miller, C. O’Hern and R. P. Behringer, *Phys. Rev. Lett.* 77, 3110 (1996).
- [34] D. Howell, R. P. Behringer and C. Veje, *Phys. Rev. Lett.* 82, 5241 (1999).
- [35] T. S. Majmudar, M. Sperl, S. Luding and R. P. Behringer, *Phys. Rev. Lett.* 98, 058001 (2007).
- [36] J. Zhang, T. S. Majmudar, M. Sperl and R. P. Behringer, *Soft Matter* 6, 2982 (2010).
- [37] E. T. Owens and K. E. Daniels, *Europhysics Letters* 94, 54005 (2011).
- [38] S. Lherminier, R. Planet, G. Simon, L. Vanel and O. Ramos, *Phys. Rev. Lett.* 113, 098001 (2014).
- [39] A. Clauset, C. R. Shalizi and M. E. Newman, *SIAM review* 51, 661 (2009).
- [40] A. Corral, *Phys. Rev. Lett.* 92, 108501 (2004).